8 Surface Consistent Probabilistic Seismic Hazard Assessment of Kolkata city

8.1 Introduction

The travel paths of the earthquake induced seismic waves in the near surface geological strata composed of weathered low velocity alluvial cover strongly affect the characteristics of the ground motion intensifying the severity of seismic hazard threat to the urban structures on the earth surface. The response of man-made structures during earthquakes is significantly controlled by two major factors *viz*. the earthquake ground motion, and the local site conditions. In general, thicker layers of soft, unconsolidated deposits tend to amplify ground motion selectively at various wave frequencies due to trapping and rebounding of the impounded energy through a complex physical phenomenon known as the overlying soil site effects over the engineering bedrock. Local topography also modifies the characteristics of the incoming waves due to the topographic effects wherein scattering and diffraction of wave energy would either amplify or de-amplify due to constructive or destructive interferences. Soil and topographic effects are usually considered under the general categorization of local site effects. The three most important phenomena that affect the ground motion amplitude at the site of interest are (1) impedance contrast between the bedrock and the soil column, (2) resonance effect from energy trapped between the bedrock and the surface, and (3) damping of the soil column. The damage patterns during the past earthquakes exhibit that soil conditions at a site may have major effects on the level of ground shaking intensity. There can be significant differences in local site conditions such as the variation in the geological formations, thickness & properties of rock/soil layers, depth of the bedrock, water table, and surface topography. Mapping of surface consistent seismic hazard at local scales incorporating the effects of local soil conditions is imperative for calculating the probability of exceeding different levels of ground motion in terms of PGA, PGV and PSA. Though the importance of site effects has been discussed in the earlier works of Seed and Idriss (1970), it is the 1985 Mexico earthquake and the 1989 Loma Prieta earthquake that drew special attention to the devastating effects that could result from site amplification thus necessitating an indepth understanding of the phenomenon. The nonlinear behavior of soils manipulating the intensity of ground shaking was demonstrated by Jarpe *et al*. (1989) who observed the reduction in amplification factor with increased intensity of shaking while comparing the amplification factors for a site on Treasure Island in San Francisco Bay for the mainshock of the 1989 Loma Prieta earthquake and its aftershocks implicating the result to reduced effective shear modulus but increased damping. Seed

et al. (1991) developed intensity dependent site amplification factors to modify the baseline "rock" peak ground acceleration (PGA) to account for site effects and estimated site specific response & design spectra. Generally the site specific amplification studies have been carried out based on geological, geophysical and geotechnical subsurface information (Kramer, 1996). The soil profile above the bedrock is developed in terms of shear wave velocity (V_s), bulk density (ρ), intrinsic shear wave damping or attenuation (Q_s) and dynamic soil properties such as shear modulus and damping versus strain curves. The behavior of soil under cyclic loading is often nonlinear and depends on several factors including amplitude of loading, number of cycles, soil type and insitu confining pressure. One dimensional site response analysis methods are routinely used to quantify the effect of soil deposits on propagated ground motions. Idriss and Seed (1968) first proposed the equivalent-linear approach for site response analysis that estimates an approximate nonlinear response through a linear analysis with soil layer properties adjusted to account for the softening during earthquake shaking. Schnabel *et al*. (1972) implemented this method in the frequency domain and developed the well known and widely used software 'SHAKE'. However in the present study the equivalent-linear concept of SHAKE has been adopted with the computation performed using DEEPSOIL (Hashash *et al*., 2011) software that facilitates both the linear and equivalent-linear analyses in the frequency domain.

8.2 Wave Propagation Analysis/Site Response

The fundamental phenomenon responsible for the amplification of ground motion in soft sediments is the entrapment of body waves. This is caused due to the impedance contrast that exists between the sediments and the bedrock. The impedance of a material is defined as

$$I = Vs * \rho \tag{8.1}$$

where I is the impedance, V_s is the shear wave velocity and ρ represents the mass density.

The shear wave velocity is considered to be the most important parameter in earthquake engineering since higher shear wave velocity represents stronger or rigid soil/sediments which behave differently under seismic loading. The shear wave velocity of the soil strata depends on its shear modulus. Several theoretical and empirical relationships exist between the shear wave velocity and the shear modulus as given by

$$G_{\max} = \rho * V_s^{\,2} \tag{8.2}$$

where $G_{\max}$ designates the shear modulus.

The impedance contrast determines the amount of wave energy that is reflected when a seismic wave passes a layer boundary where the material properties get altered. The trapped waves

interfere at the boundary causing amplification of ground motion and inducing resonance patterns. The multiple reflections within the layers cause constructive interferences at resonance periods. The resonance effect does not occur at one specific frequency, but at several ones, resulting in site and material specific resonance patterns.

The one dimensional wave propagation analysis is widely used for ground response analysis/ soil amplification studies for the estimation of ground motion at the earth surface. The following assumptions are made during the analysis:

(a) The soil layers are horizontal, homogeneous and extend to infinity.

(b) The ground surface is level.

(c) The incident earthquake motions which are considered to be spatially uniform and propagates vertically.

The estimation of transfer functions is the key parameter in ground response analysis. It requires solving the wave propagation equation for 1-D soil model. The function provides the amplification or de-amplification factor with respect to the bedrock motion which is used as an input to compute the surface level ground motion. The basic wave equation for a uniform damped soil is as per Kramer, (1996) which is

$$\rho \frac{\delta^2 u}{\delta t^2} = G \frac{\delta^2 u}{\delta z^2} + \eta \frac{\delta^3 u}{\delta z^2 \delta t} \tag{8.3}$$

The solution of the wave equation for horizontal displacement caused to the soil deposit at j^{th} layer as depicted in Figure 8.1 can be expressed as

$$u(z_j, t) = (A_j e^{ik^*_j z_j} + B_j e^{-ik^*_j z_j}) e^{i\omega t} \tag{8.4}$$

where A and B represent the amplitudes in its complex form of the upward wave and k^* represent the complex wave number which is related to shear modulus (G), damping ratio (ζ) and density (ρ) of the soil strata, defined as

$$k^* = \omega / v_s^*, \quad v_s^* = \sqrt{\frac{G^*}{\rho}}, \quad G^* = G(1 + i2\xi) \tag{8.5}$$

where G^* and v_s^* are complex shear modulus and complex shear wave velocity respectively and ω represents the wave frequency.

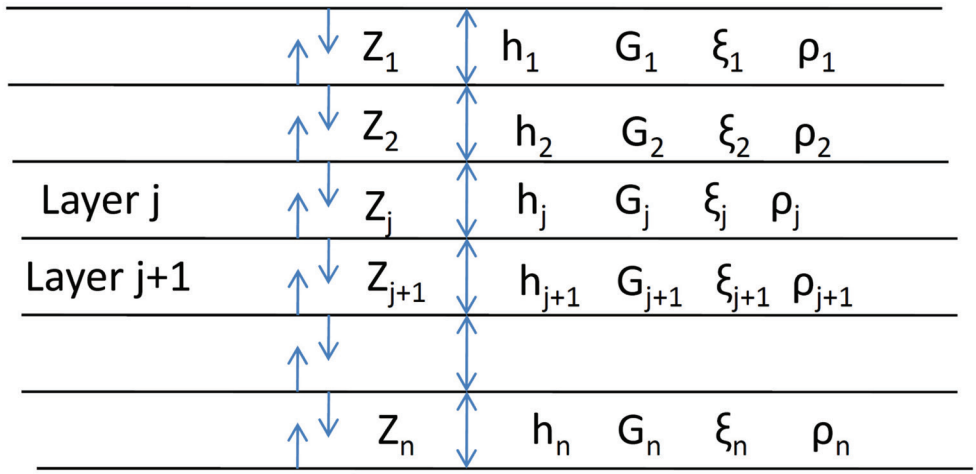

Figure 8.1 **Nomenclature for theoretical wave propagation.**

The wave amplitudes are calculated using recursive formulations developed by maintaining compatibility of displacement and shear stress at the layer boundaries and are given as (Kramer, 1996)

$$A_{j+1} = \frac{1}{2} A_j (1+\alpha^*_j) e^{ik^*_j h_j} + \frac{1}{2} B_j (1-\alpha^*_j) e^{-ik^*_j h_j} \tag{8.6}$$

$$B_{j+1} = \frac{1}{2} A_j (1-\alpha^*_j) e^{ik^*_j h_j} + \frac{1}{2} B_j (1+\alpha^*_j) e^{-ik^*_j h_j} \tag{8.7}$$

where α^* represent the complex impedance ratio at the boundary between layer j and j+1.

Applying equation (8.6) and (8.7) recursively for j=1,2,3….n, the coefficients A_{j+1} and B_{j+1} can be related to A_j and B_j as

$$A_{j+1} = a_{j+1}(\omega) A_1 \quad \ddot{u}_{j+\ddot{u}} = \quad {}_{j+}(\omega) \tag{8.8}$$

Where the functions a_{j+1} and b_{j+1} represent the effect of wave interaction that occurs at the interface of the (j+1)th layer. Thus the transfer function between i^{th} and j^{th} layers can be expressed as

$$T_f(\omega) = \frac{a_i(\omega) + b_i(\omega)}{a_j(\omega) + b_j(\omega)} \tag{8.9}$$

The response spectrum at the interface between these two layers is computed by multiplying the Fourier amplitude spectrum of the input rock motion by the transfer function in its spectral form.

In equivalent-linear site response analysis, the nonlinear effect of the soil/sediment is approximated by modifying the linear elastic properties of the soil based on the induced strain level. Thus, the strain compatible shear modulus and damping ratio values are iteratively calculated based on the computed strain level. The steps followed in this analysis are as follows (Kramer, 1996):

(1) Initial estimation of G and ζ for each layer.

(2) The strain transfer function calculated for each of the layers.

(3) The estimated G and ζ used for the computation of ground response, including the time histories of shear strain for each layer.

(4) Effective shear strain in each layer determined from the maximum shear strain in the time history.

(5) The strain compatible shear modulus and damping ratio recalculated based on the new estimates of the effective strain within each layer.

(6) The new nonlinear properties (G and ζ) compared with the values obtained in the previous iteration and an error calculated thereof. If the error for all layers falls below a defined threshold the calculation terminates.

Thus, with the use of updated nonlinear properties the transfer function is generated for each soil layer. The Fourier series of the output motion at ground surface is represented as a convolution of the Fourier series of the input (bedrock) motion and the transfer function.

The overall process of wave propagation from seismic bedrock to engineering bedrock through elastic half and then through the overlying soil column to the surface is schematically represented in Figure 8.2.

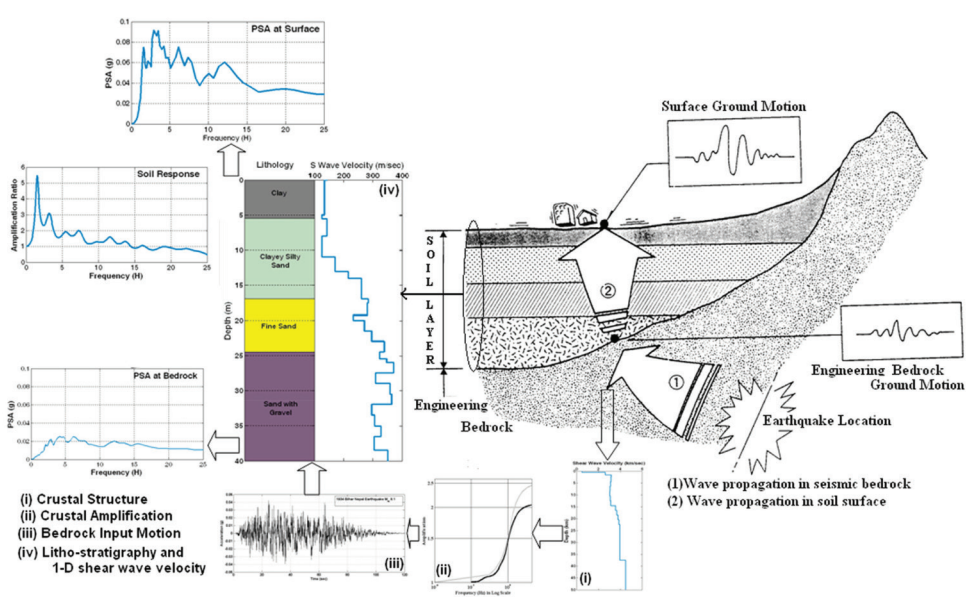

Figure 8.2 **Schematic illustration of wave propagation from seismic bedrock to engineering bedrock through an elastic half and then through the overlying soil column to the surface (Modified after Nath, 2007).**

Different strategies have been proposed by various researchers to account for soil nonlinearity behavior using numerical techniques. The nonlinear hysteretic model developed by Iwan (1967) & Mroz (1967) was initially implemented by Bardet *et al*., (2000) in the EERA code & NERA code (Bardet and Tobita, 2001) which later on were modified and implemented in the DEEPSOIL software (Hashash *et al*., 2008) for dynamic nonlinear analyses. In the present study one dimensional ground response analysis has been performed using the graphical user interface in DEEPSOIL following the steps as depicted in Figure 8.3. In the standard protocol a soil profile with the corresponding physical and shear properties is an input through which the ground motion at the engineering bed rock is propagated. For a typical site response analysis the soil profile is excited by the horizontal component of the ground motion.

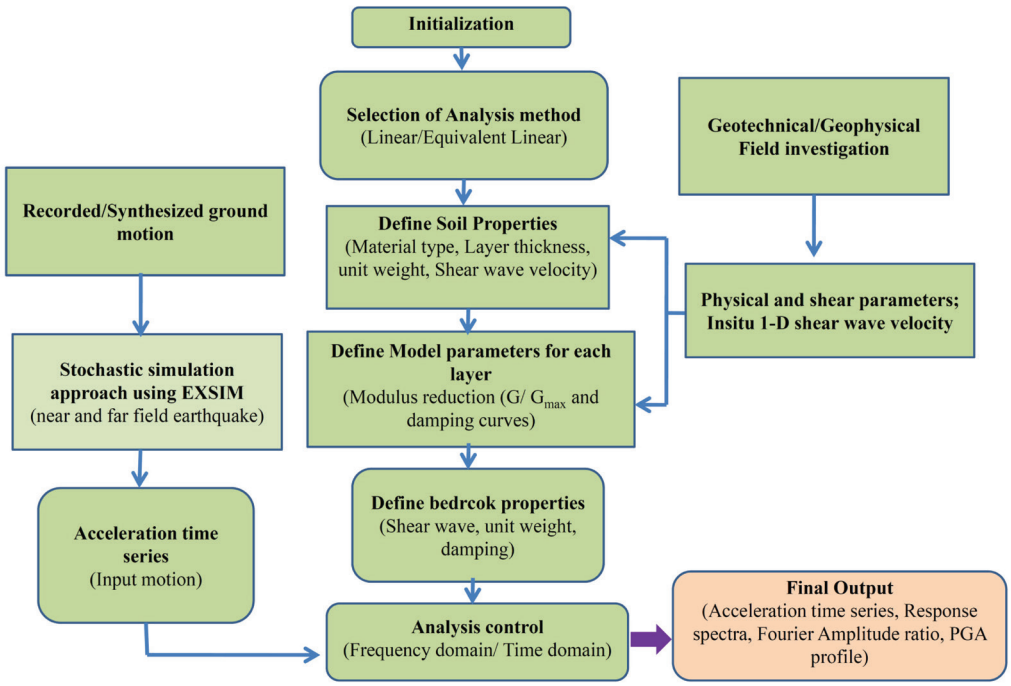

Figure 8.3 **Flowchart for 1-D nonlinear site response analysis through DEEPSOIL software.**

8.2.1 Bedrock Input Motion Synthesis

The input ground acceleration is synthesized using stochastic simulation software package EXSIM at engineering bedrock for both the near and far source earthquakes *viz*. 1934 Bihar-Nepal earthquake of M_w 8.1, 1918 Srimangal earthquake of M_w 7.6, 1897 Shillong earthquake of M_w 8.1 and 1930 Dhubri earthquake of M_w 7.1. The source functions of these earthquakes extracted from published literatures are given in Table 8.1. The representative time history as simulated for 1934 Bihar-Nepal earthquake of M_w 8.1 at Saltlake in Kolkata is presented in Figure 8.4.

Table 8.1 **Parameters used for Strong Ground motion simulation**

Parameter	1934 Bihar-Nepal earthquake[(a)]	1918 Srimangal earthquake[(b)]	1897 Shillong earthquake[(c)]	1930 Dhubri earthquake[(b)]
Strike	285º	45°	112°	4°
Dip	6º	77°	50°	45°
Focal depth (km)	20	14	35	60
Source (Location)	27.55°N, 87.09°E	23.8°N, 90.1°E	26.0°N, 91.0°E	25.0°N, 89.6°E
Magnitude (M_w)	8.1	7.6	8.1	7.1
Stress (bar)	275	159	159	159
Crustal density (g/cm3)	2.7	2.7	2.7	2.7
Shear wave velocity, β (km/s)	3.8	3.8	3.8	3.8
Quality factor	$400f^{0.48}$	$224f^{0.93}$	$400f^{0.48}$	$224f^{0.93}$
Kappa	0.02	0.02	0.02	0.02
Geometrical spreading	1/R (R<100 km) $1/R^{0.5}$ (R>100 km)			
Windowing function	Saragoni and Hart (1974)			
Damping	5%			
(a) Nath *et al.* (2010), (b) Raghukanth and Dash (2010), (c) Hough and Bilham (2008)				

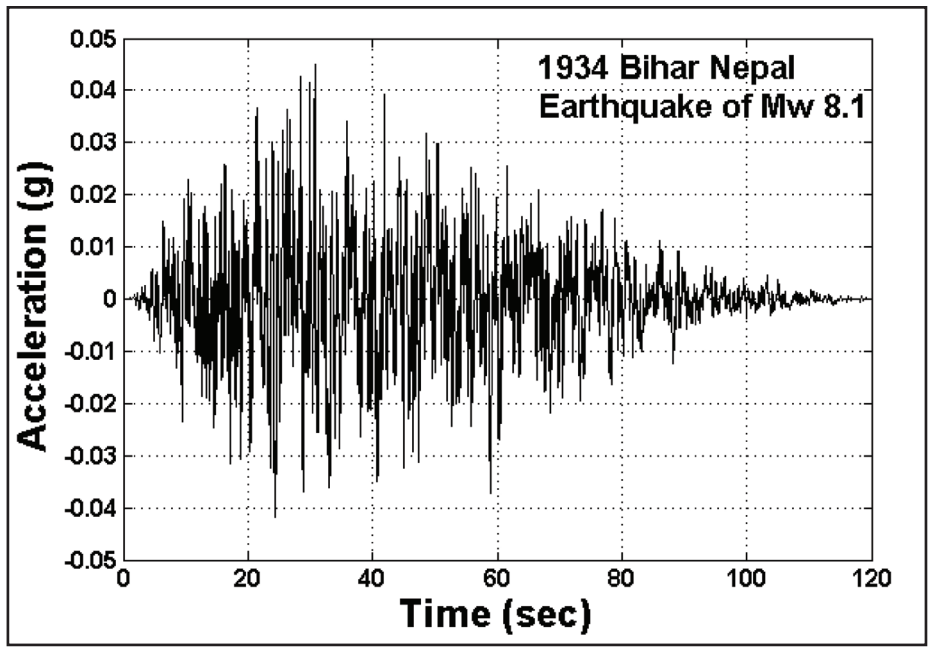

Figure 8.4 **Representative acceleration time history for 1934 Bihar-Nepal earthquake at bedrock level at Saltlake in Kolkata.**

8.2.2 Definition of Input Model

The rock properties defining the rigid half space or an elastic half space have to be specified in the analysis. The rigid half space is selected if ground motion is used from in-hole motion commonly obtained by vertical array survey. In most of the common situations the elastic half space is recommended, which represent the transmitting boundary at the base of the soil column and uses the bedrock ground motion as input parameter. In the elastic half space the shear wave velocity (or modulus), unit weight and damping ratio of the half space at rock site have been specified. On this elastic half space 1-D soil profile is stacked through which the input bedrock motions is propagated for spectral response estimation and site response analysis. The soil properties of the column includes the soil type, thickness of the layer, unit weight and shear wave velocity for each layer as illustrated in Figure 8.5 at Saltlake in Kolkata out of a total of 654 geotechnical borehole locations, 85 MASW sites, 1200 microtremor survey locations and 18 insitu downhole seismic survey sites spread over ~435 km^2 area in the City. The detailed Geophysical and Geotechnical investigation conducted in Kolkata for site characterization as well as site response analysis have been illustrated greater details in Chapters 5 and 6.

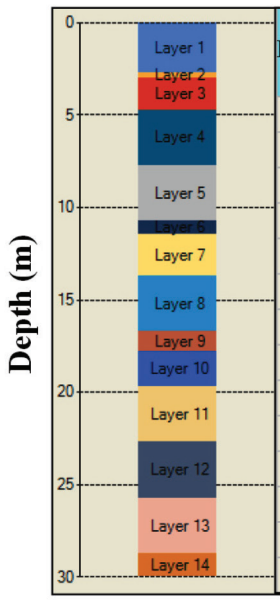

Layer	Layer Name	Thickness (m)	Unit Weight kN/m^3	Shear Velocity (m/s)
1	Light grey silty fine sand (filled up)	2.7	16.9	115.0618
2	Dark grey clayey silt	0.3	17.1	108.6363127
3	Dark grey clayey silt	1.725	17.2	104.6165232
4	Dark grey clayey silt	3	17	140.0283683
5	Dark grey clayey silt	3	17.4	180.3502134
6	Dark grey clayey silt	0.775	17.5	218.8269931
7	Bluish grey silty clay with boulders	2.225	17.4	213.8978527
8	Bluish grey silty clay with boulders	3	17.7	214.0427633
9	Bluish grey silty clay with boulders	1.075	18.5	212.149027
10	Light yellow with brownush patches silt	1.925	18.6	208.9898781
11	Light yellow with brownush patches silt	3	18.9	274.0375165
12	Light yellow with brownush patches silt	3	19	324.6792
13	Light yellow with brownush patches silt	3	19.2	365.8982
14	Light yellow with brownush patches silt	1.275	20.8	390.2075

Figure 8.5 **Input soil profile and model properties for sample location in Saltlake, Kolkata.**

The soil behavior under irregular cyclic loading is modeled using modulus reduction (G/G_{max}) and damping ratio vs. strain curves. The DEEPSOIL module uses a set of material curves for defining the modulus reduction and damping ratio for different types of soils. In case of sands the

appropriate modulus reduction curves are defined based on effective vertical stress by selecting an appropriate option in the module. In case of clays, the effective vertical stress and plasticity index are required to be defined for estimating the modulus reduction and damping curves. Representative degradation curves for sand as proposed by Seed and Idriss (1970) used in the present study is shown in Figure 8.6. Soil behaves nonlinearly as the damping ratio increases wherein secant modulus decreases with an increase in the cyclic shear strain.

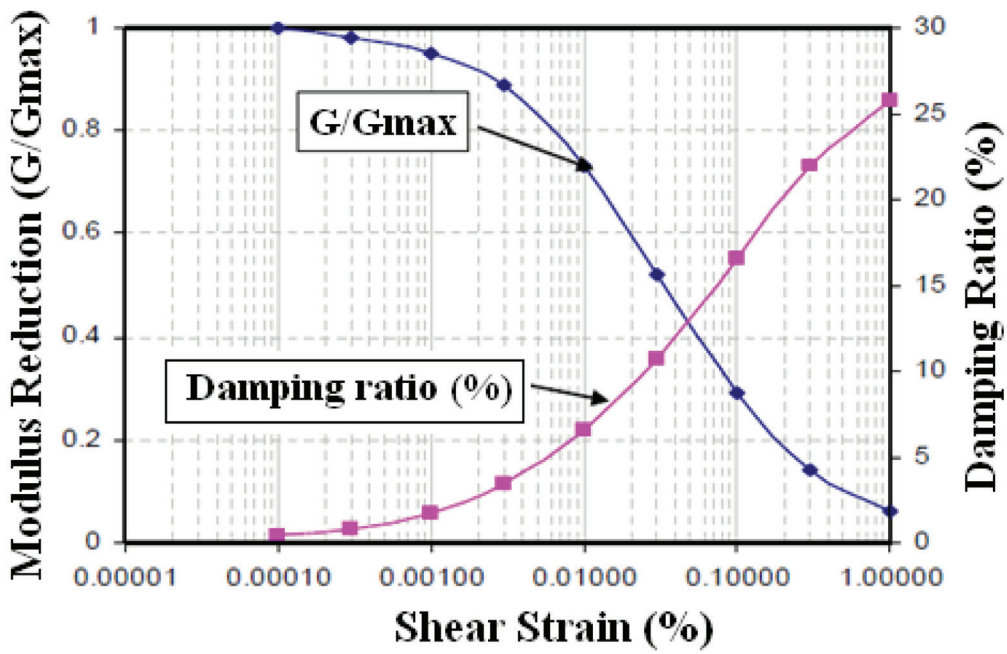

Figure 8.6 **Shear modulus and damping ratio curves for sand (Seed and Idriss, 1970).**

8.2.3 Results: Illustration and Discussion

The site response analysis has been performed at all the borehole locations with the employment of appropriate bedrock motions and soil column to simulate ground motion at the surface. Representative Response Spectra at the surface, Fourier Amplitude ratio and PGA variation along the soil profile at Saltlake of Kolkata is displayed in Figure 8.7.

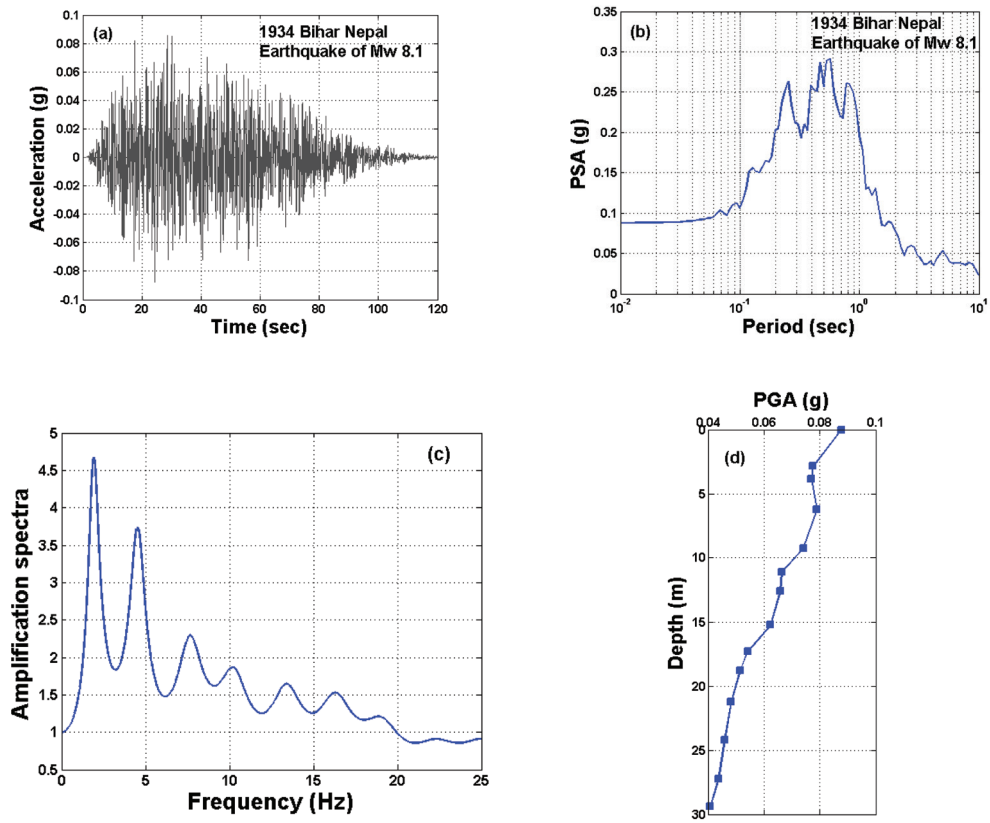

Figure 8.7 **Sample output using DEEPSOIL at Saltlake of Kolkata: (a) Acceleration at the surface, (b) Response spectra at the surface, (c) Amplification spectra/ Amplitude ratio, and (d) Depth wise PGA variation along the soil profile.**

The representative illustrations of propagation of synthesized bedrock motion through 1-D lithostratigraphic soil column to the surface at selective locations *viz*. Nicco Park, Shibpur, Brabourne Street, Rajarhat in Kolkata are depicted in Figure 8.8 to Figure 8.11. It is evident from these diagrams that the soil column at each location altered the bedrock ground motion significantly wherein it got amplified at predominant frequencies of all the sites in question due to the trapping up of the seismic energy in the low velocity soil column and rebounding of the same.

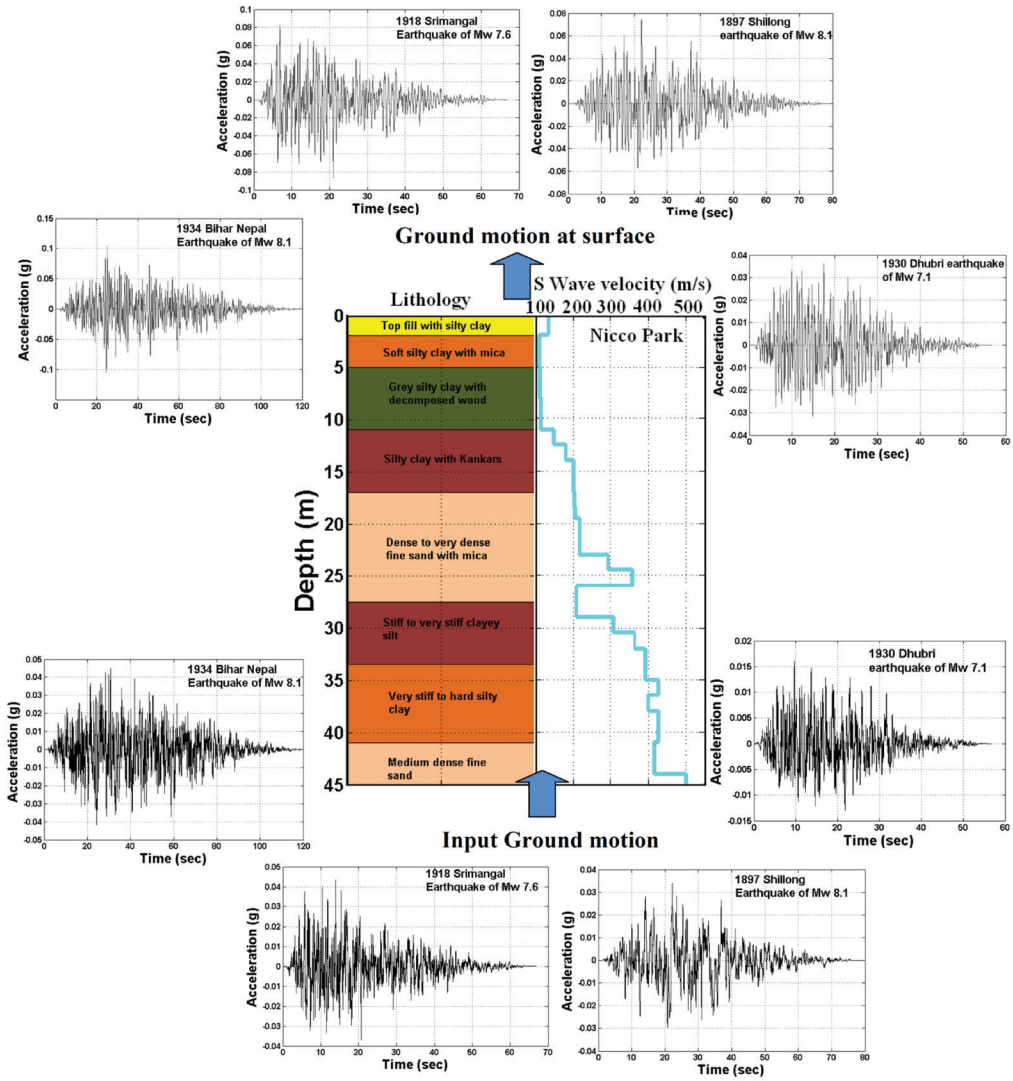

Figure 8.8 Lithostratigraphy and 1-D shear wave velocity depth profile used for DEEPSOIL analysis at Nicco Park in Kolkata.

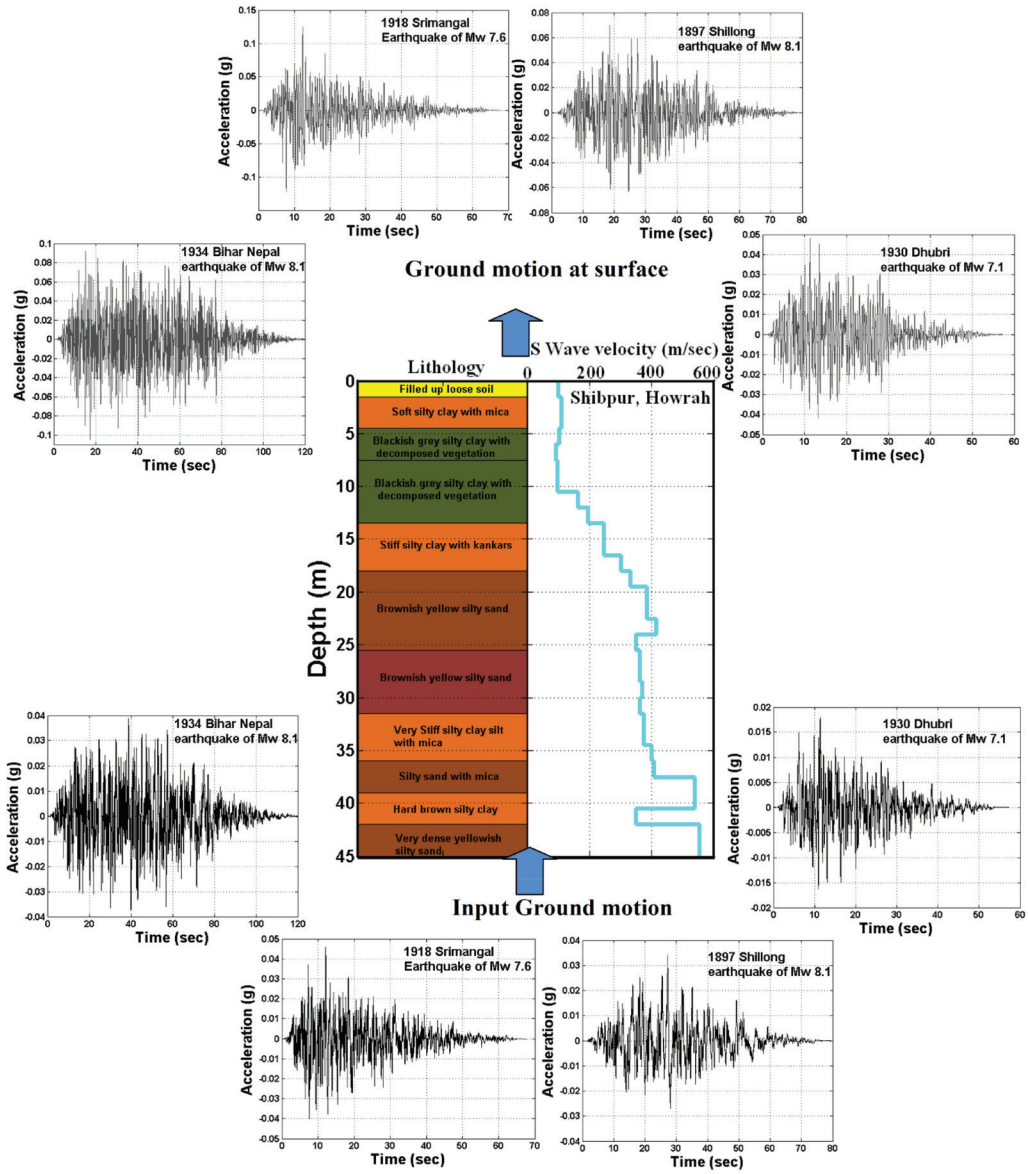

Figure 8.9 Lithostratigraphy and 1-D shear wave velocity depth profile used for DEEPSOIL analysis at Shibpur, Howrah in Kolkata.

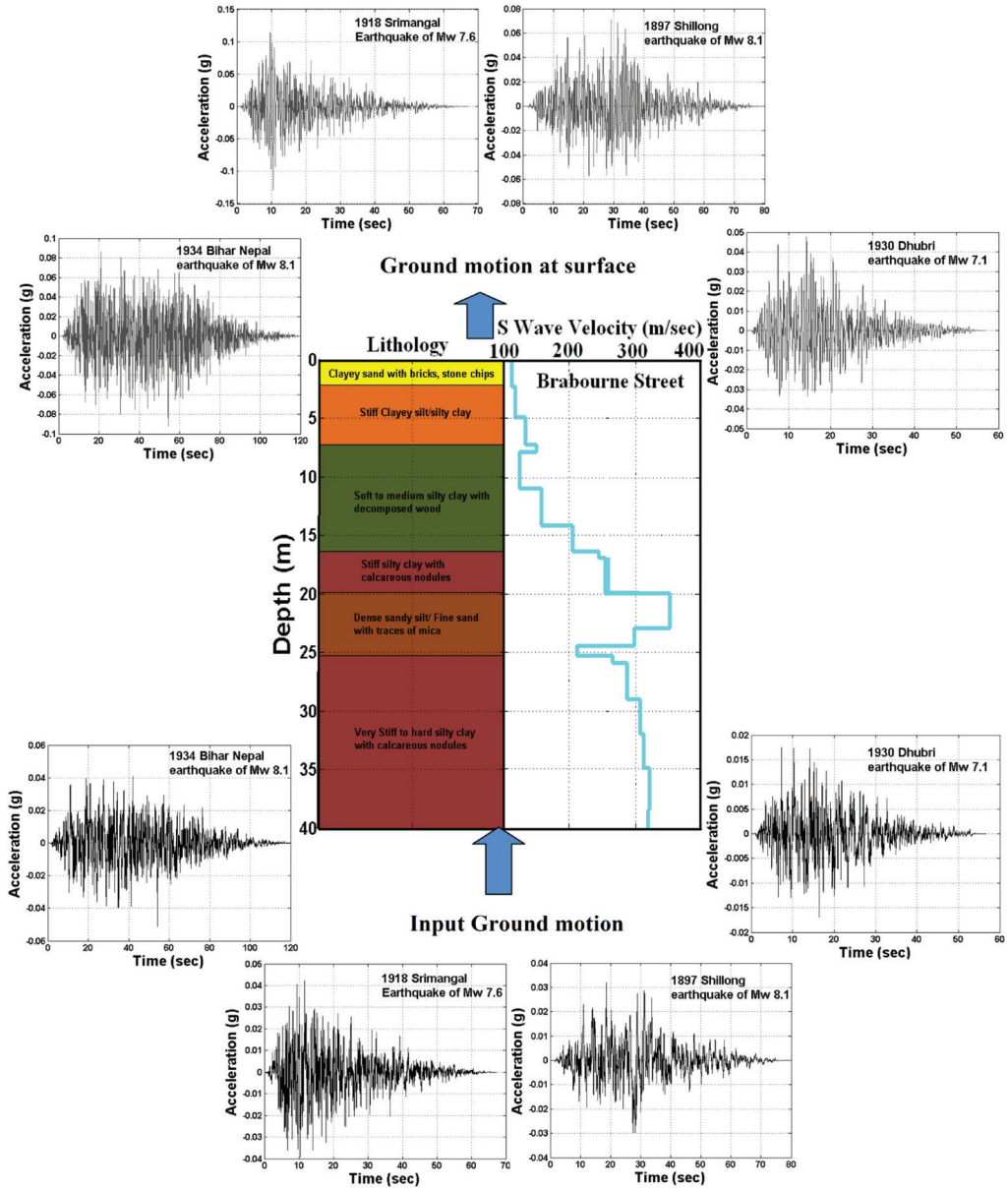

Figure 8.10 Lithostratigraphy and 1-D shear wave velocity depth profile used for DEEPSOIL analysis at Brabourne Street in Kolkata.

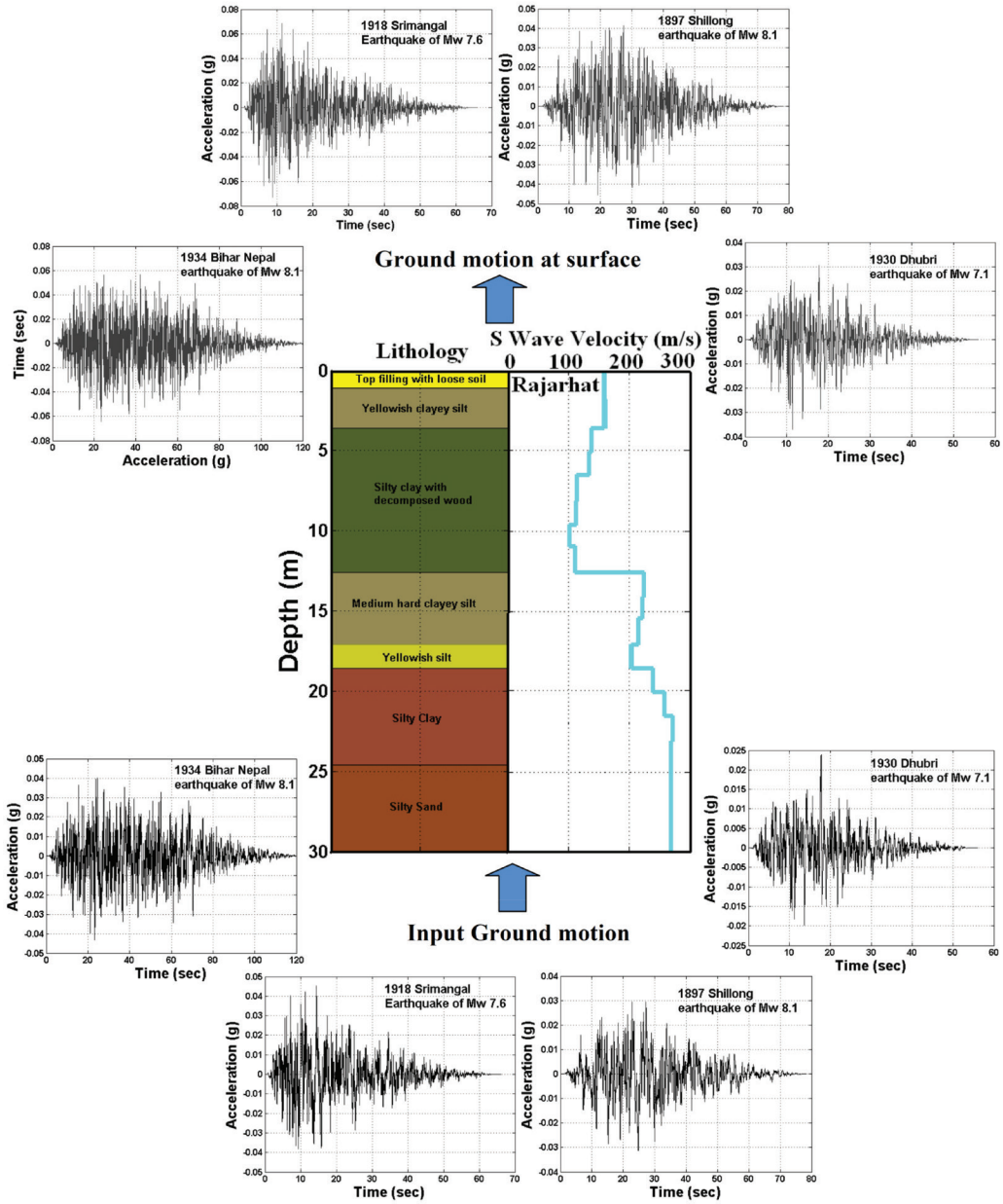

Figure 8.11 Lithostratigraphy and 1-D shear wave velocity depth profile used for DEEPSOIL analysis at Rajarhat in Kolkata.

The nonlinear effect of the alluvial soil on the propagated ground motion is measured by Amplification spectra which are considered as one of the governing factors in the design of new structures and performance assessment of the existing ones. As already discussed, the site amplification is estimated as the ratio between the bedrock response spectra and the surface level response spectra which are represented by Fourier Amplitude Ratio or the Amplification spectra at both the levels. The Amplification spectra thus define the unit impulse response of the soil strata under the seismic impact. Figure 8.12 presents the Amplification spectral curves within a frequency band encompassing the fundamental and higher order modes at selective locations *viz*. Rajarhat, Dum Dum, Paikpara, Shibaji Sangha, Dasnagar, Shibpur, Maheshtala, Thakurpukur, Tollygunge, Sonarpur, Narendrapur, Bagdoba, Kasba, Brabourne Road, Rajabazar, Saltlake in Kolkata out of a total of 654 borehole locations considering the four near and far-field earthquakes mentioned earlier.

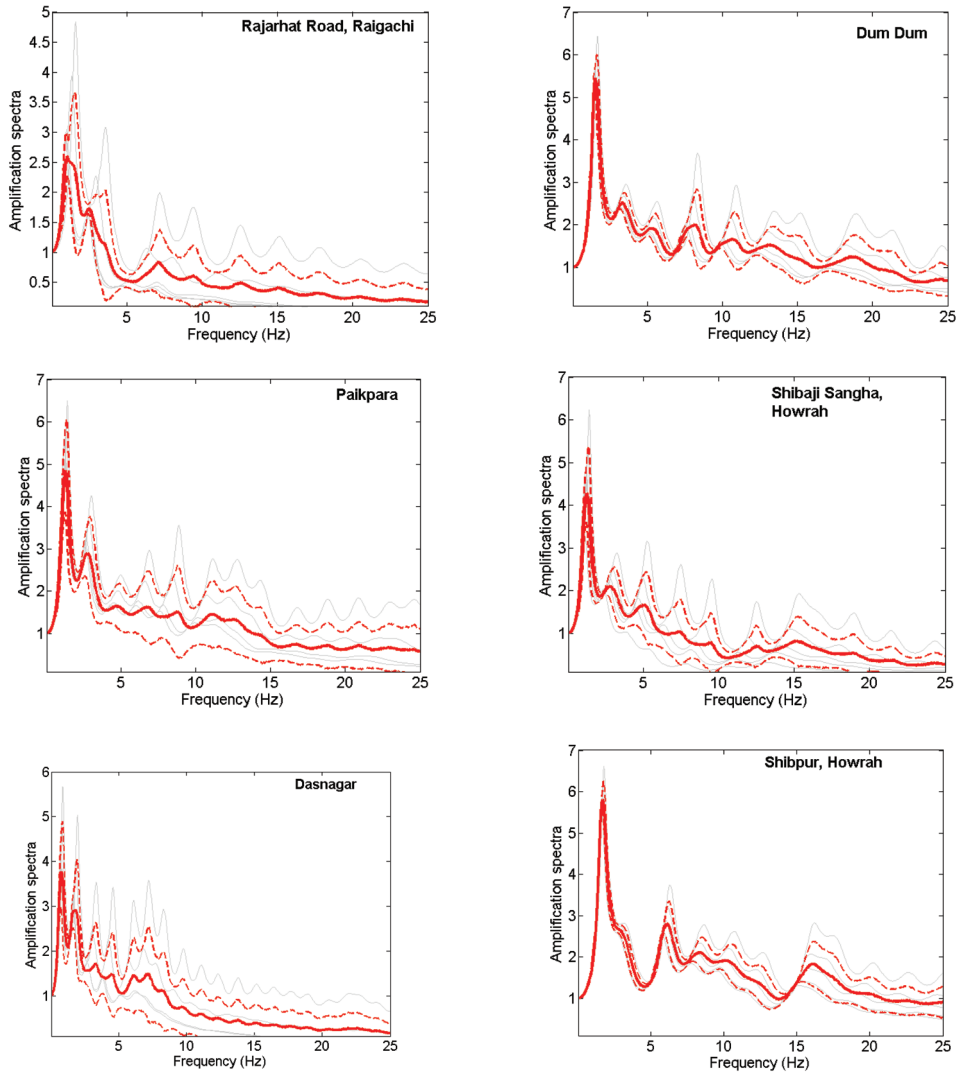

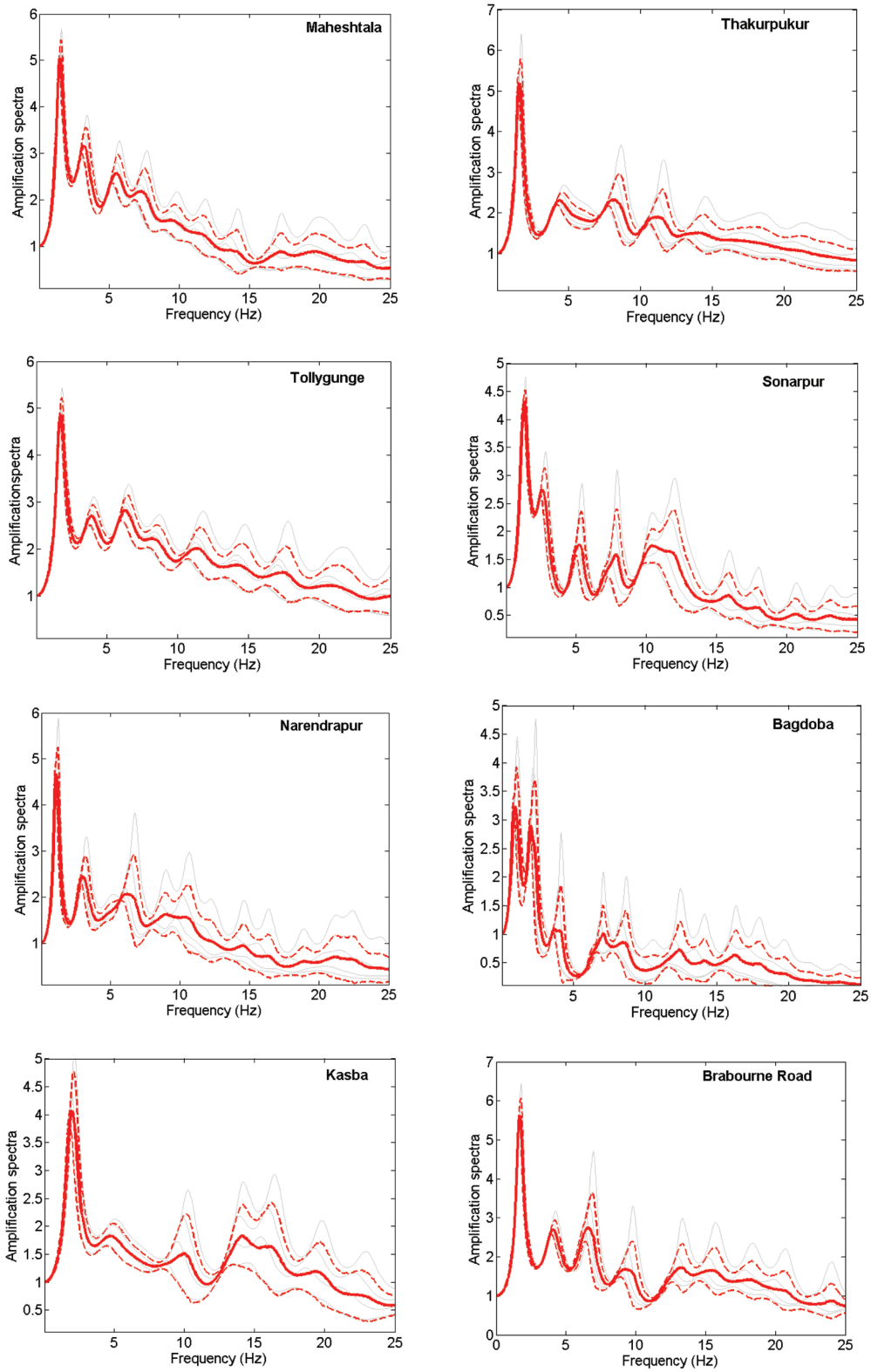
Maheshtala
Thakurpukur
Tollygunge
Sonarpur
Narendrapur
Bagdoba
Kasba
Brabourne Road
Amplification spectra
Amplificationspectra
Frequency (Hz)

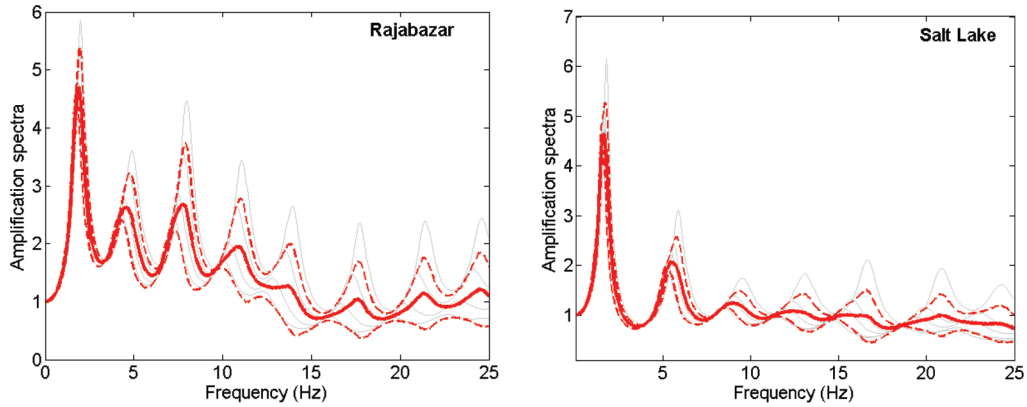

Figure 8.12 **Representative Amplification spectral curves within a frequency band encompassing the fundamental and higher order modes along with standard deviation (σ) at selective borehole locations in Kolkata city.**

8.3 Probabilistic Seismic Hazard Assessment at Surface Level

Surface consistent seismic hazard in terms of PGA and PSA at 0.2 sec, 0.3 sec and 1.0 sec have been computed for both 10% and 2% probability of being exceeded in 50 years by propagating those at engineering bedrock (already discussed in Chapter 4) through 1-D soil column at each grid point of the City having shear wave velocity information wherein site amplification got convolved with the bedrock ground motion. In otherwords the acceleration time series generated in the probabilistic seismic hazard assessment at bedrock has been used as input ground motion propagated through 1-D shear wave velocity profile at each of 1957 locations defined by calibrating 654 borehole site information with 85 location MASW based surface measurements, 1200 location microtremor recordings and 18 downhole refraction survey in the City (discussed in greater details in Chapters 5 and 6). The resulting spatial distribution of PGA at 1957 locations in the city of Kolkata for 10% probability of exceedance in 50 years is displayed on GIS platform in Figure 8.13 (a) with its error distribution in terms of standard deviation shown in Figure 8.13 (b). The same for 2% probability of exceedance in 50 years at 1957 locations distributed spatially on GIS platform is shown in Figure 8.13 (c) along with its error distribution in terms of standard deviation shown in Figure 8.13 (d). While the variation in PGA for 10% probability of exceedance in 50 years at surface level depicts a range of 0.14g to 0.34g in the City, it got escalated to a range of 0.3g to 0.66g depicting almost doubling of the hazard level for the return period of 2475 years with 2% probability of exceedance in 50 years.

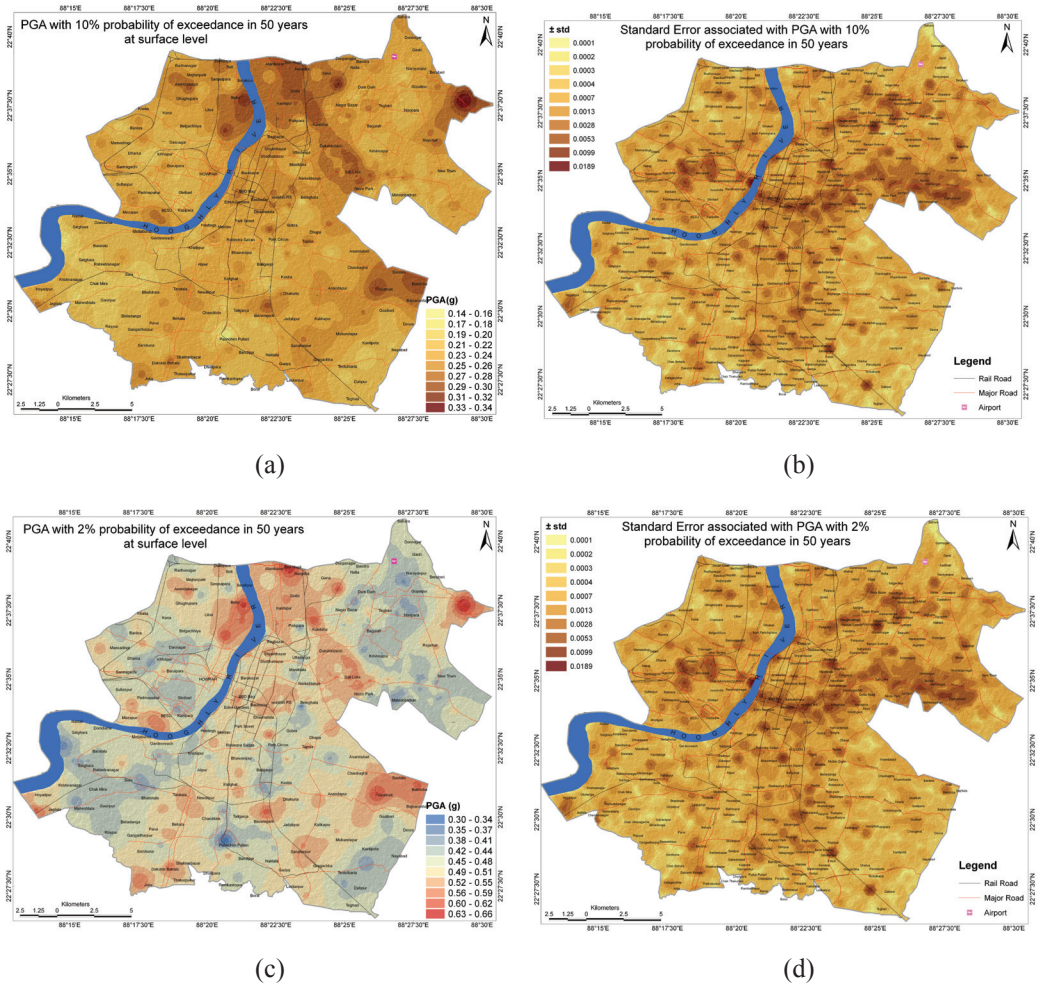

Figure 8.13 **(a) Spatial distribution of PGA for 10% probability of exceedance in 50 years at surface level in Kolkata, (b) Error distribution in terms of standard deviation associated with PGA for 10% probability of exceedance in 50 years, (c) Spatial distribution of PGA for 2% probability of exceedance in 50 years at surface level in Kolkata, and (d) Error distribution in terms of standard deviation associated with PGA for 2% probability of exceedance in 50 years.**

PSA at both the short period 0.2 sec and long period 1.0 sec are essential for the generation of design response spectra while PSA at 0.3 sec and 1.0 sec are needed for risk and loss estimation studies using SELENA and HAZUS protocols. The spatial distribution of PSA at 0.2 sec in the city of Kolkata for 10% probability of exceedance in 50 years is displayed on GIS platform in Figure 8.14(a) with its error distribution in terms of standard deviation shown in Figure 8.14(b). The same for 2% probability of exceedance in 50 years distributed spatially on GIS platform is shown in Figure 8.14(c) along with its error distribution in terms of standard deviation shown in Figure 8.14(d). While the variation in PSA at 0.2 sec for 10% probability of exceedance in 50 years at surface depicts a range of 0.26g to 1.08g in the City, it got escalated to a range of 0.55g to 2.1g depicting almost doubling of the hazard level for the return period of 2475 years with 2% probability of exceedance in 50 years.

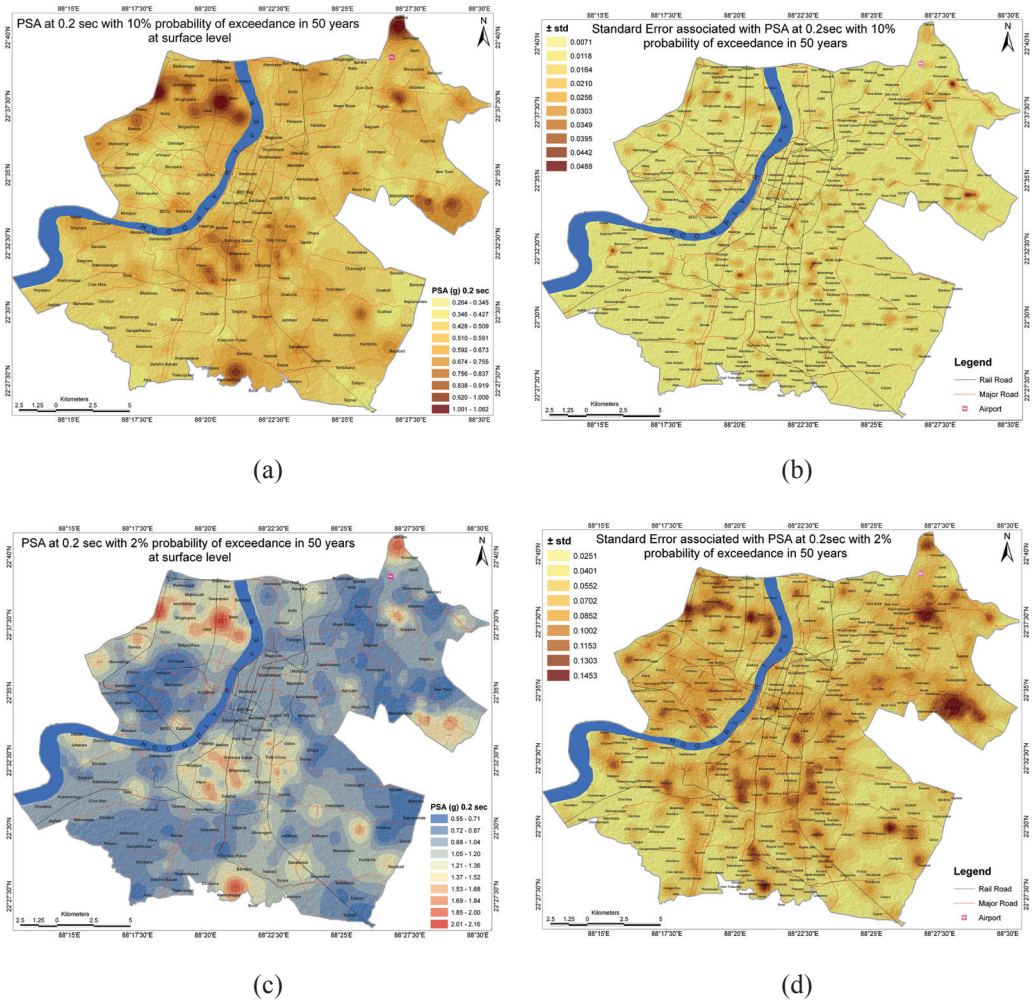

Figure 8.14 **(a) Spatial distribution of PSA at 0.2 sec for 10% probability of exceedance in 50 years at surface level in Kolkata, (b) Error distribution in terms of standard deviation associated with PSA at 0.2 sec for 10% probability of exceedance in 50 years, (c) Spatial distribution of PSA at 0.2 sec for 2% probability of exceedance in 50 years at surface level in Kolkata, and (d) Error distribution in terms of standard deviation associated with PSA at 0.2 sec for 2% probability of exceedance in 50 years.**

The spatial distribution of PSA at 0.3 sec in the city of Kolkata for 10% probability of exceedance in 50 years is displayed on GIS platform in Figure 8.15(a) with its error distribution in terms of standard deviation shown in Figure 8.15(b). The same for 2% probability of exceedance in 50 years distributed spatially on GIS platform is shown in Figure 8.15(c) along with its error distribution in terms of standard deviation shown in Figure 8.15(d). While the variation in PSA at 0.3 sec for 10% probability of exceedance in 50 years at surface depicts a range of 0.22g to 0.95g in the City, it got escalated to the range of 0.49g to 1.82g depicting almost doubling of the hazard level for the return period of 2475 years with 2% probability of exceedance in 50 years.

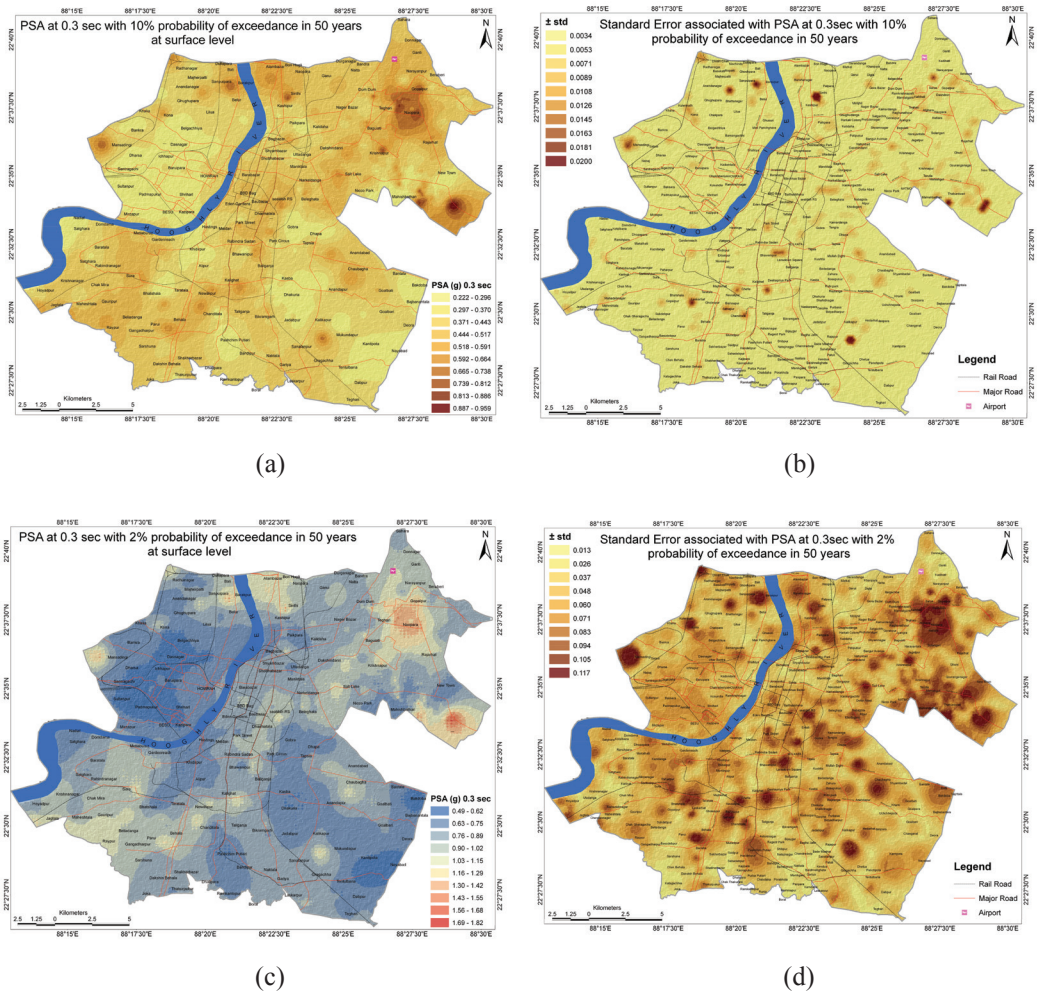

Figure 8.15 **(a) Spatial distribution of PSA at 0.3 sec for 10% probability of exceedance in 50 years at surface level in Kolkata, (b) Error distribution in terms of standard deviation associated with PSA at 0.3 sec for 10% probability of exceedance in 50 years, (c) Spatial distribution of PSA at 0.3 sec for 2% probability of exceedance in 50 years at surface level in Kolkata, and (d) Error distribution in terms of standard deviation associated with PSA at 0.3 sec for 2% probability of exceedance in 50 years.**

The spatial distribution of PSA at 1.0 sec in the city of Kolkata for 10% probability of exceedance in 50 years is displayed on GIS platform in Figure 8.16(a) with its error distribution in terms of standard deviation shown in Figure 8.16(b). The same for 2% probability of exceedance in 50 years distributed spatially on GIS platform is shown in Figure 8.16(c) along with its error distribution in terms of standard deviation shown in Figure 8.16(d). While the variation in PSA at 1.0 sec for 10% probability of exceedance in 50 years at surface depicts a range of 0.06g to 0.24g in the City, it got escalated to the range of 0.19g to 0.62g for 2% probability of exceedance in 50 years.

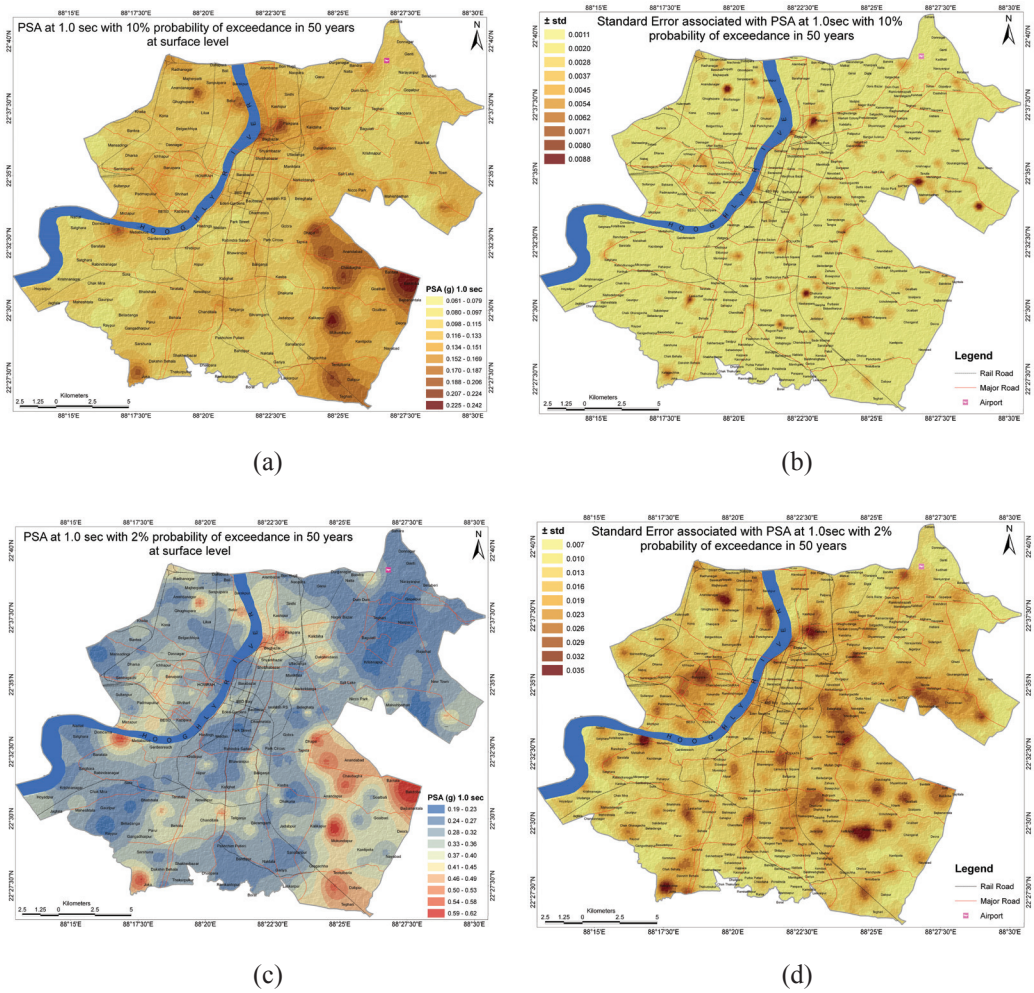

Figure 8.16 **(a) Spatial distribution of PSA at 1.0 sec for 10% probability of exceedance in 50 years at surface level in Kolkata, (b) Error distribution in terms of standard deviation associated with PSA at 1.0 sec for 10% probability of exceedance in 50 years, (c) Spatial distribution of PSA at 1.0 sec for 2% probability of exceedance in 50 years at surface level in Kolkata, and (d) Error distribution in terms of standard deviation associated with PSA at 1.0 sec for 2% probability of exceedance in 50 years.**

8.4 Design Response Spectra in Kolkata

The design response spectrum is defined as the smoothened plot of maximum acceleration as a function of frequency or time period for a specific damping ratio due to earthquake excitations at the base of a single degree of freedom system. These are essential for analyzing the performance of

structures under earthquake loading which is applied for the design of structures and development of lateral force in building codes. In all the current seismic codes, the earthquake actions are represented in the form of a design response spectrum in terms of PGA and PSA. The scheme given by IBC (2006; 2009) scales the design spectrum by two spectral ordinates at 0.2 sec and 1.0 sec corresponding to the short and long periods, respectively. The amplification factors for different site classes defined by National Earthquake Hazard Reduction Program (NEHRP) for two different spectral periods are listed in Tables 8.2 and 8.3.

Table 8.2 **Amplification factors for acceleration response spectra at 0.2 sec (after IBC, 2006). S_s denotes spectral acceleration at 0.2 sec period**

Site class	Mapped spectral acceleration (g)				
	$S_s \leq 0.25$	$S_s = 0.50$	$S_s = 0.75$	$S_s = 1.00$	$S_s \geq 1.25$
A	0.8	0.8	0.8	0.8	0.8
B	1.0	1.0	1.0	1.0	1.0
C	1.2	1.2	1.1	1.0	1.0
D	1.6	1.4	1.2	1.1	1.0
E	2.5	1.7	1.2	0.9	0.9

Table 8.3 **Amplification factors for acceleration response spectra at 1.0 sec (after IBC, 2006). S_l denotes spectral acceleration at 1.0 sec period**

Site class	Mapped spectral acceleration (g)				
	$S_l \leq 0.25$	$S_l = 0.50$	$S_l = 0.75$	$S_l = 1.00$	$S_l \geq 1.25$
A	0.8	0.8	0.8	0.8	0.8
B	1.0	1.0	1.0	1.0	1.0
C	1.7	1.6	1.5	1.4	1.3
D	2.4	2.0	1.8	1.6	1.5
E	3.5	3.2	2.8	2.4	2.4

The procedure followed in the design response as given by IBC (2006; 2009) is as follows:

(1) Compute the maximum considered earthquake spectral response acceleration at 0.2 sec and 1.0 sec periods as

$$S_{MS} = F_a S_s \tag{8.10}$$

$$S_{ML} = F_v S_l \tag{8.11}$$

F_a and F_v correspond to the amplification factors for acceleration response spectra at 0.2 sec and 1.0 sec periods, respectively as listed in Tables 8.2 and 8.3. S_s and S_l denote the spectral accelerations at the respective periods.

(2) Compute the design basis earthquake spectral response acceleration at 0.2 sec and 1.0 sec periods as

$$S_{DS} = 2/3\ S_{MS} \tag{8.12}$$

$$S_{DL} = 2/3\ S_{ML} \tag{8.13}$$

(3) Determine the characteristic time-periods as

$$T_0 = 0.2\ S_{DL}/S_{DS} \tag{8.14}$$

$$T_S = S_{DL}/S_{DS} \tag{8.15}$$

(4) Construct the design response spectra as

$$Sa = \begin{cases} 0.6(S_{DS}/T_0)T + 0.4S_{DS}, & T \le T_0 \\ S_{DS}, \quad T \ge T_0\ and & T \le T_s \\ S_{DL}/T, & T \ge T_s \end{cases} \tag{8.16}$$

Where S_a is the design spectral response acceleration and T is the fundamental time-period of the structure.

The 5% damped design response spectra have been generated using PSA at 1.0 sec and 0.2 sec with 10% probability of exceedence in 50 years following the International Building Code (IBC, 2009) for the selected locations/landmarks *viz*. Rajarhat, Saltlake, Dum Dum, Park Circus, Park Street, Jadavpur, Alipur, Maheshtala, Howrah, Shibpur, Liluah, Garia in the city of Kolkata at both the bedrock and surface levels as presented in Figure 8.17 which exhibit an increase in the design values in the updating of the existing building codes implying a probable escalation in urbanization cost throughout the City.

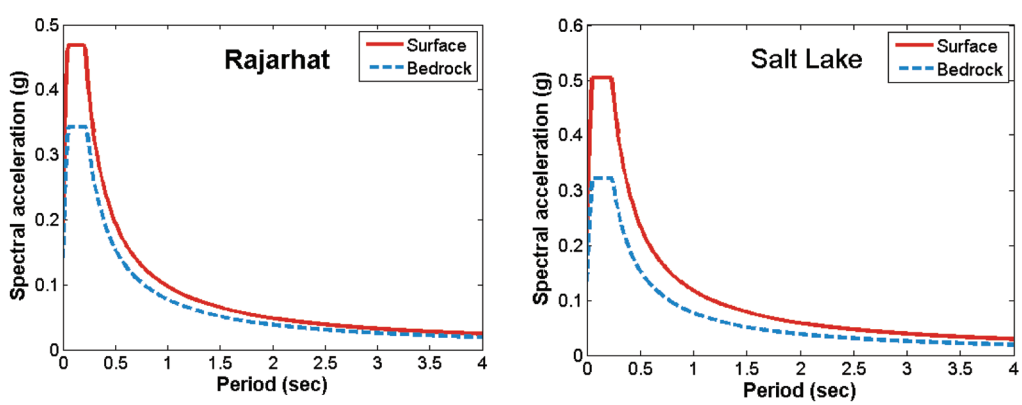

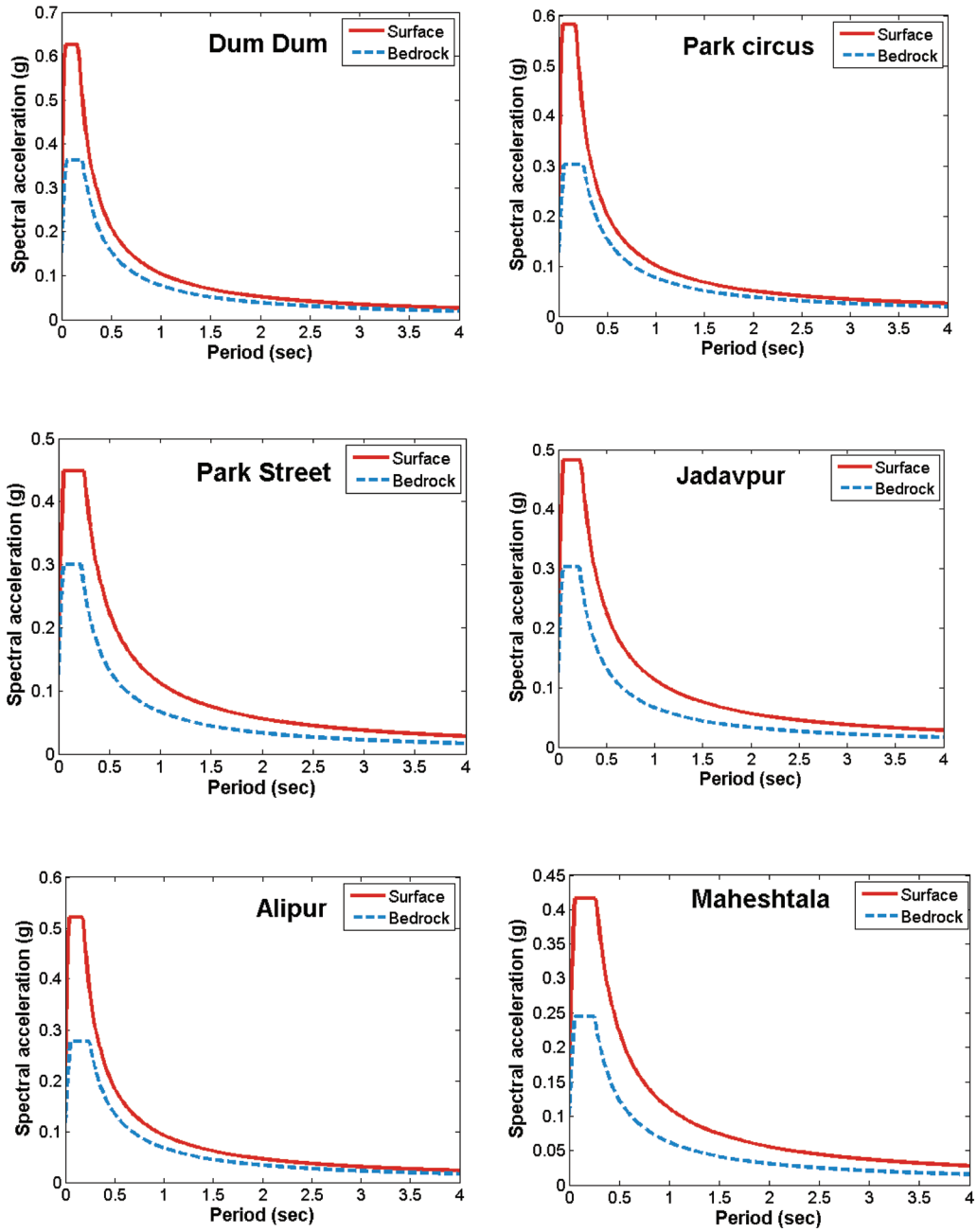
Dum Dum
Park circus
Park Street
Jadavpur
Alipur
Maheshtala
Surface
Bedrock
Spectral acceleration (g)
Period (sec)

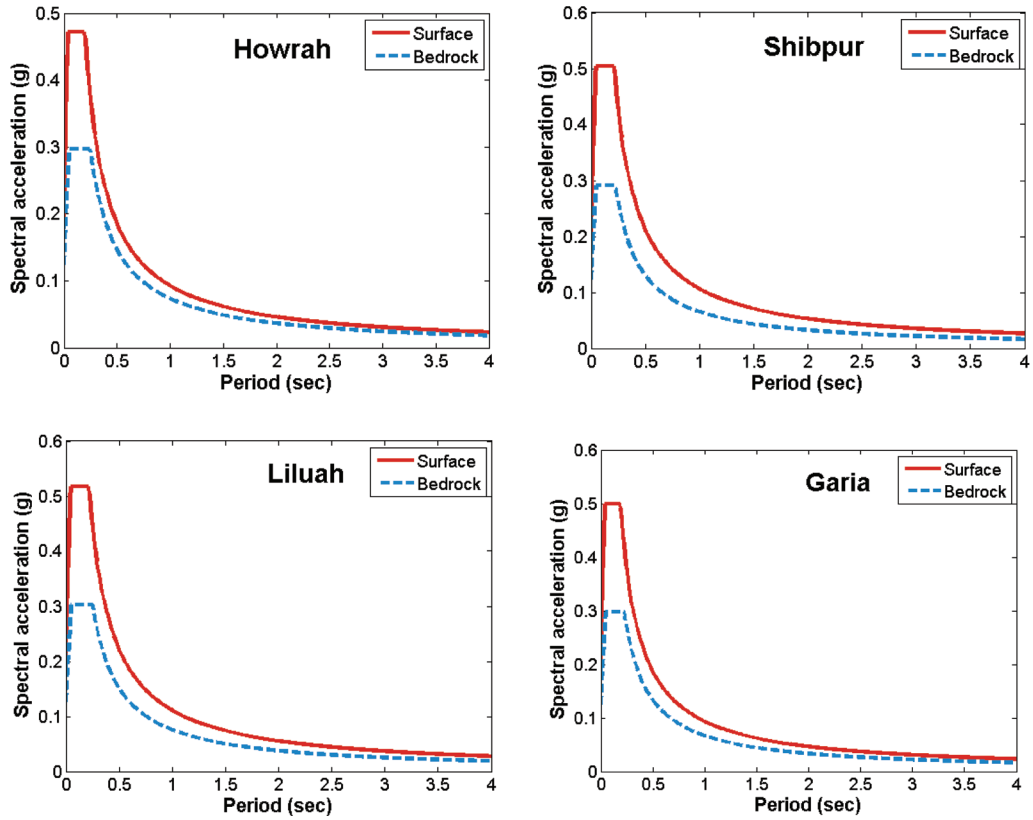

Figure 8.17 **Design response spectra (5% damped) generated using PSA at 1.0 and 0.2 sec with 10% probability of exceedance in 50 years for selected locations/landmarks in Kolkata at both the engineering bedrock and surface levels.**

8.5 Concluding Remarks

The ground response analysis is an important step in the seismic hazard assessment of an earthquake-prone district. The city of Kolkata being overlain by thick alluvium deposits ranging in some places to even 7.5 km thickness provides a suitable case for nonlinear analysis of ground response characterizing the site effect and related phenomena. The ground motion amplification pattern is evidently controlled by local geology, geomorphology and the physical and shear parameters of the underlying lithostatigraphy of the sedimentary formation which eventually influence the seismic hazard at the surface of the City necessitating appropriate safety regulations to mitigate its effect.